Metasurfaces based dual wavelength diffractive lenses

Omri Eisenbach,* Ori Avayu, Ran Ditcovski and Tal Ellenbogen

Department of Physical Electronics, Fleischman Faculty of Engineering, Tel Aviv University, Tel Aviv 69978, Israel
**omrie@mail.tau.ac.il*

Abstract: We demonstrate experimentally and by simulations a method for using thin nanostructured plasmonic metasurfaces to design diffractive Fresnel zone plate lenses that focus pairs of wavelengths to a single focal point. The metasurfaces are made of tightly packed cross and rod shaped optical nanoantennas with strong polarization and wavelength selectivity. This selectivity allows multiplexing two different lenses with low spectral crosstalk on the same substrate and to address any superposition of the two colors at the focus of the lenses by controlling the polarization of light. This concept can open the door to use ultrathin diffractive lenses in fluorescence microscopy and in stimulated emission depletion microscopy.

OCIS codes: (160.3918) Metamaterials; (260.5430) Polarization; (050.1965) Diffractive lenses; (250.5403) Plasmonics; (080.1010) Aberrations (global).

References and Links

1. A. V. Kildishev, A. Boltasseva, and V. M. Shalaev, "Planar photonics with metasurfaces," Science **339**(6125), 1232009 (2013).
2. N. Yu and F. Capasso, "Flat optics with designer metasurfaces," Nat. Mater. **13**(2), 139–150 (2014).
3. I. Richter, P. C. Sun, F. Xu, and Y. Fainman, "Design considerations of form birefringent microstructures," Appl. Opt. **34**(14), 2421–2429 (1995).
4. Z. Bomzon, G. Biener, V. Kleiner, and E. Hasman, "Radially and azimuthally polarized beams generated by space-variant dielectric subwavelength gratings," Opt. Lett. **27**(5), 285–287 (2002).
5. U. Levy, C.-H. Tsai, L. Pang, and Y. Fainman, "Engineering space-variant inhomogeneous media for polarization control," Opt. Lett. **29**(15), 1718–1720 (2004).
6. J. Yang, X. Xiao, C. Hu, W. Zhang, S. Zhou, and J. Zhang, "Broadband surface plasmon polariton directional coupling via asymmetric optical slot nanoantenna pair," Nano Lett. **14**(2), 704–709 (2014).
7. T. Ellenbogen, K. Seo, and K. B. Crozier, "Chromatic plasmonic polarizers for active visible color filtering and polarimetry," Nano Lett. **12**(2), 1026–1031 (2012).
8. L. Novotny and N. van Hulst, "Antennas for light," Nat. Photonics **5**(2), 83–90 (2011).
9. P. Biagioni, J.-S. Huang, and B. Hecht, "Nanoantennas for visible and infrared radiation," Rep. Prog. Phys. **75**(2), 024402 (2012).
10. J. Dorfmüller, R. Vogelgesang, W. Khunsin, C. Rockstuhl, C. Etrich, and K. Kern, "Plasmonic nanowire antennas: experiment, simulation, and theory," Nano Lett. **10**(9), 3596–3603 (2010).
11. P. Mühlschlegel, H.-J. Eisler, O. J. F. Martin, B. Hecht, and D. W. Pohl, "Resonant optical antennas," Science **308**(5728), 1607–1609 (2005).
12. M. W. Knight, L. Liu, Y. Wang, L. Brown, S. Mukherjee, N. S. King, H. O. Everitt, P. Nordlander, and N. J. Halas, "Aluminum plasmonic nanoantennas," Nano Lett. **12**(11), 6000–6004 (2012).
13. J. Goodman, *Introduction to Fourier Optics* (McGraw-hil, 2008).
14. J. Vila-Comamala, S. Gorelick, E. Färm, C. M. Kewish, A. Diaz, R. Barrett, V. A. Guzenko, M. Ritala, and C. David, "Ultra-high resolution zone-doubled diffractive X-ray optics for the multi-keV regime," Opt. Express **19**(1), 175–184 (2011).
15. S. Wang, T. Yuan, E. D. Walsby, R. J. Blaikie, S. M. Durbin, D. R. S. Cumming, J. Xu, and X.-C. Zhang, "Characterization of T-ray binary lenses," Opt. Lett. **27**(13), 1183–1185 (2002).
16. E. T. Rogers, J. Lindberg, T. Roy, S. Savo, J. E. Chad, M. R. Dennis, and N. I. Zheludev, "A super-oscillatory lens optical microscope for subwavelength imaging," Nat. Mater. **11**(5), 432–435 (2012).
17. D. Fattal, J. Li, Z. Peng, M. Fiorentino, and R. G. Beausoleil, "Flat dielectric grating reflectors with focusing abilities," Nat. Photonics **4**(7), 466–470 (2010).
18. L. Verslegers, P. B. Catrysse, Z. Yu, J. S. White, E. S. Barnard, M. L. Brongersma, and S. Fan, "Planar lenses based on nanoscale slit arrays in a metallic film," Nano Lett. **9**(1), 235–238 (2009).

#228831 - $15.00 USD Received 9 Dec 2014; revised 18 Jan 2015; accepted 19 Jan 2015; published 9 Feb 2015

19. F. M. Huang, T. S. Kao, V. A. Fedotov, Y. Chen, and N. I. Zheludev, "Nanohole array as a lens," Nano Lett. **8**(8), 2469–2472 (2008).
20. L. Lin, X. M. Goh, L. P. McGuinness, and A. Roberts, "Plasmonic lenses formed by two-dimensional nanometric cross-shaped aperture arrays for Fresnel-region focusing," Nano Lett. **10**(5), 1936–1940 (2010).
21. Y. Gao, J. Liu, K. Guo, Y. Gao, and S. Liu, "A side-illuminated plasmonic planar lens," Opt. Express **22**(1), 699–706 (2014).
22. X. Chen, L. Huang, H. Mühlenbernd, G. Li, B. Bai, Q. Tan, G. Jin, C.-W. Qiu, S. Zhang, and T. Zentgraf, "Dual-polarity plasmonic metalens for visible light," Nat Commun **3**, 1198 (2012).
23. X. Ni, S. Ishii, A. V. Kildishev, and V. M. Shalaev, "Ultra-thin, planar, Babinet-inverted plasmonic metalenses," Light Sci. Appl. **2**(4), e72 (2013).
24. F. Aieta, P. Genevet, M. A. Kats, N. Yu, R. Blanchard, Z. Gaburro, and F. Capasso, "Aberration-free ultrathin flat lenses and axicons at telecom wavelengths based on plasmonic metasurfaces," Nano Lett. **12**(9), 4932–4936 (2012).
25. L. Novotny, "Effective wavelength scaling for optical antennas," Phys. Rev. Lett. **98**(26), 266802 (2007).
26. Y. Montelongo, J. O. Tenorio-Pearl, W. I. Milne, and T. D. Wilkinson, "Polarization switchable diffraction based on subwavelength plasmonic nanoantennas," Nano Lett. **14**(1), 294–298 (2014).
27. L. Wang, T. Li, R. Y. Guo, W. Xia, X. G. Xu, and S. N. Zhu, "Active display and encoding by integrated plasmonic polarizer on light-emitting-diode," Sci Rep **3**, 2603 (2013).
28. W. T. Chen, K.-Y. Yang, C.-M. Wang, Y.-W. Huang, G. Sun, I.-D. Chiang, C. Y. Liao, W.-L. Hsu, H. T. Lin, S. Sun, L. Zhou, A. Q. Liu, and D. P. Tsai, "High-efficiency broadband meta-hologram with polarization-controlled dual images," Nano Lett. **14**(1), 225–230 (2014).
29. O. Avayu, O. Eisenbach, R. Ditcovski, and T. Ellenbogen, "Optical metasurfaces for polarization-controlled beam shaping," Opt. Lett. **39**(13), 3892–3895 (2014).
30. F. Monticone, N. M. Estakhri, and A. Alù, "Full control of nanoscale optical transmission with a composite metascreen," Phys. Rev. Lett. **110**(20), 203903 (2013).
31. Y. Yifat, M. Eitan, Z. Iluz, Y. Hanein, A. Boag, and J. Scheuer, "Highly efficient and broadband wide-angle holography using patch-dipole nanoantenna reflectarrays," Nano Lett. **14**(5), 2485–2490 (2014).

Nanotechnology enables to construct ordered materials consisting of nanoscale sub-wavelength inclusions. The optical properties of these materials can be controlled by the type of the sub-wavelength inclusions and by their arrangements and can be based on metal-dielectric nanostructures [1, 2] or all-dielectric nanostructures [3–5]. These materials are commonly called optical metamaterials or metasurfaces due to their unique properties which cannot always be found in natural materials.

Some of the metasurfaces which were demonstrated are based on excitation of localized surface plasmon resonances (LSPR) on metal nanostructures embedded in dielectrics [1,2,6,7]. In the LSPR the metal nanostructures can be considered as optical nanoantennas (ONATs) due to their ability to efficiently receive optical radiation at specific frequencies and focus it to the near field, or transmit near field electromagnetic energy to the far field [8–12]. In addition, the light scattering and absorption cross-sections of the ONATs grow considerably to dimensions much larger than their physical size. Therefore light at the LSPR frequency can be manipulated efficiently by the metasurface. It was shown that by changing the shape of the ONATs their LSPR can be tuned from the ultraviolet to the infrared regimes [10]. This enables designing ONAT-based metasurfaces that fit a broad spectral range and opens new possibilities to create novel, ultrathin, and integrated optical components.

The most useful optical components are lenses which can be found in a wide variety of devices. The common way to construct lenses is to use refraction by curved surfaces. However refractive lenses have some drawbacks. For example, due to the curvature of the surface, the lenses are bulky and limit miniaturization of devices. In addition it is hard to produce refractive lenses with high numerical apertures due to the appearance of large spherical and chromatic aberrations. These aberrations can be corrected, but on the expense of size, weight and cost of the lens.

An alternative way to focus light is to use diffractive optical elements (DOEs) [13]. Lenses based on DOEs are wildly used in the industry from high end optics for astronomy and microscopy to low end laser pointers. One of the biggest drawbacks of diffractive lenses is that they suffer from very large chromatic aberrations, as shown in Fig. 1, and therefore they are designed to work at a specific single wavelength. For applications that require

#228831 - $15.00 USD Received 9 Dec 2014; revised 18 Jan 2015; accepted 19 Jan 2015; published 9 Feb 2015

polychromatic light, e.g. fluorescence microscopy and most of the imaging applications, DOE based lenses cannot be used.

Figure 1(a) shows a calculation of the distance to focus of a diffractive binary Fresnel zone plate lens (FZP) that was designed to focus light at a wavelength of 620 nm to 1 mm away from the lens. For lenses with focal lengths much larger than the effective wavelength (f>>λ), f can be calculated by $f = \frac{R_1^2}{\lambda}$ where R_1 is the radius of the first ring of the FZP. It can be seen that each wavelength is focused to a different position in space. Figure 1(b) shows the output of beam propagation simulation of the same lens demonstrating how light at 620 nm is focused to 1 mm away from the lens while light at 460 nm is focus to ~1.4 mm away from the lens. To examine it we produced a one dimensional FZP lens, shown in Fig. 1(c), and measured the propagation of light after the lens. The measurements, shown in Fig. 1(d), illustrate that each wavelength is focused to a different point in space. Therefore applications which require focusing or imaging with more than one wavelength cannot benefit from such a lens. This gives a strong motivation to develop DOEs which can focus multiple wavelengths to the same focal spot. One promising way to achieve it is to use optical metasurfaces.

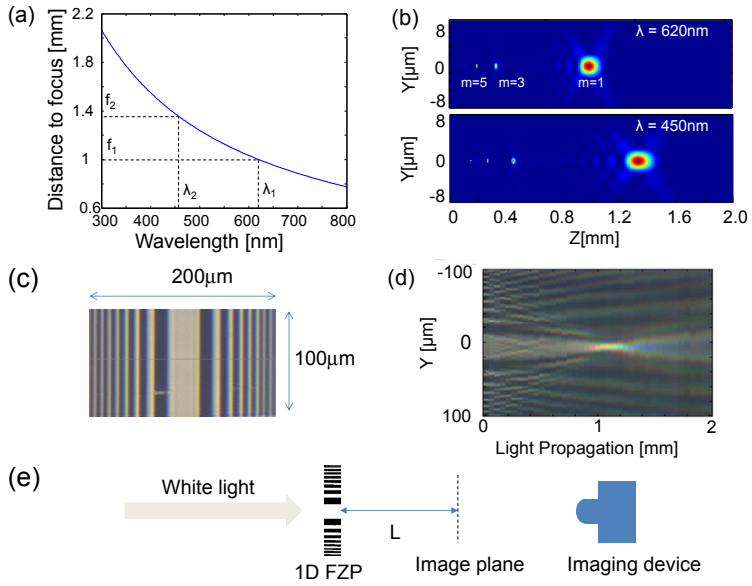

Fig. 1. Chromatic aberrations induced by conventional FZP. (a) Calculated focal distance vs. wavelength of FZP designed to focus 620 nm at 1 mm focal distance. (b) Beam propagation simulation results of light focused by a 2D FZP designed for 620 nm with f = 1 mm. (c) Optical microscope image of fabricated conventional 1D binary FZP made from Aluminum stripes on glass. (d) Measurement of light propagation after the 1D binary FZP shown in (c). (e) Illustration of test setup.

The use of nanostructured surfaces for implementing DOEs in general, and especially diffractive lenses, has been demonstrated with sub-wavelength gratings [14,15], nano slits and holes [16–20]. The concept of ONATs was also used for building diffractive lenses [2, 21–24] which were ultrathin spherical aberration free and possibly with high NA. This demonstrates the potential of nanotechnology for the construction of new optical elements. However in these works the lenses or diffractive elements were designed for single wavelength and were not meant to correct the chromatic aberrations when two or more wavelengths need to be address.

#228831 - $15.00 USD Received 9 Dec 2014; revised 18 Jan 2015; accepted 19 Jan 2015; published 9 Feb 2015

In this work we experimentally demonstrate an implementation of diffractive metasurface-based FZP (mFZP) that corrects chromatic aberrations at pairs of wavelengths in the visible regime. The design of the mFZP is based on merging two independent zone plate lenses, in the same metasurface, one for each polarization. Our experimental results agree with the simulation results and pave the way towards manufacturing multi-wavelength and functional diffractive lenses.

The metasurfaces that are used to construct the mFZP in this work consist of cross shaped and rod shaped ONATs which have a strong polarization and wavelength selectivity. It was shown that the effective resonance wavelength of ONATs follows an empirical linear relation [25]: $\lambda_{eff} = n_1 + n_2\lambda/\lambda_p$, where n_1 and n_2 are coefficients that depend on the dielectric environment and the shape of the ONAT and λ_p is the plasma wavelength. It was shown specifically that this relation is maintained also for cross shaped ONATs [7]. In addition the anisotropic shape of these ONATs adds a strong local polarization selectivity. Since the transmission function of the ONAT depends on its resonance, by creating metasurfaces out of wavelength and polarization selective ONATs the total transmission function can be presented by:

$$T(\varphi,\lambda,x,y) = T_V(\lambda,x,y)\sin^2(\varphi) + T_H(\lambda,x,y)\cos^2(\varphi) \tag{1}$$

where $T_V(\lambda,x,y)$ and $T_H(\lambda,x,y)$ are the spatial transmission response of the metasurface to vertically and horizontally polarized light, λ is the free space wavelength, and φ is the angle between the polarization of incoming light and the x axis. This gives the ability to encode different independent DOEs into the wavelength space and polarization space which are separated by the ONATs response [7, 26–29]. Here we use it to correct the chromatic aberrations of FZP at two different wavelengths. The functionality of conventional FZP and mFZP is illustrated in Figs. 2(a) and 2(b) respectively.

The mFZP in this work relies on "mixing" two independent FZPs. One FZP is designed to focus horizontally polarized light at wavelength of 460 nm to 1 mm away from the lens. This functionality is encoded on the horizontal polarization response of the metasurface. The second FZP is designed to focus vertically polarized light at 650 nm to 1 mm away from the lens. This functionality is encoded on the vertical polarization response of the metasurface.

A binary FZP can be described by the following transmission function

$$U = \frac{1}{2}\left(1 + sign\left(\cos\left(\frac{2\pi}{\lambda^f} * \frac{x^2+y^2}{2f}\right)\right)\right) \tag{2}$$

where λ^f is the wavelength that will be focused after length f, and can be taken as the operation wavelength. In order to construct mFZP that corrects chromatic aberrations of pairs of wavelengths, two different lenses with U_V and U_H have to be calculated, with two different operation wavelengths $\lambda^f_{V,H}$. The polarization-dependent transmission functions can then be described by:

$$T_V(\lambda,x,y) = \begin{cases} t_V(\lambda) & U_V(x,y) = 0 \\ 1 & U_V(x,y) = 1 \end{cases} \qquad T_H(\lambda,x,y) = \begin{cases} t_H(\lambda) & U_H(x,y) = 0 \\ 1 & U_H(x,y) = 1 \end{cases} \tag{3}$$

where $t_{V,H}(\lambda)$ is the spectral transmission response of the metasurface at the two polarizations. The total transmission function is then calculated by Eq. (1). This divides the operation of the mFZP to different spectral regimes and different polarizations as calculated and presented in Fig. 2(c). In comparison to a regular FZP (shown in Fig. 1 (a)) the distance to focus is now divided into two regimes according to the source polarization, and it can be seen how pairs of wavelengths now share the same focal length. Figure 2(d) shows the output of

#228831 - $15.00 USD Received 9 Dec 2014; revised 18 Jan 2015; accepted 19 Jan 2015; published 9 Feb 2015

beam propagation simulation of the metasurface based lens showing how light at 650 nm and light at 460 nm are now focused to the same spot in space (in comparison to Fig. 1(b)). This demonstrates the correction of chromatic aberrations at the two working wavelengths.

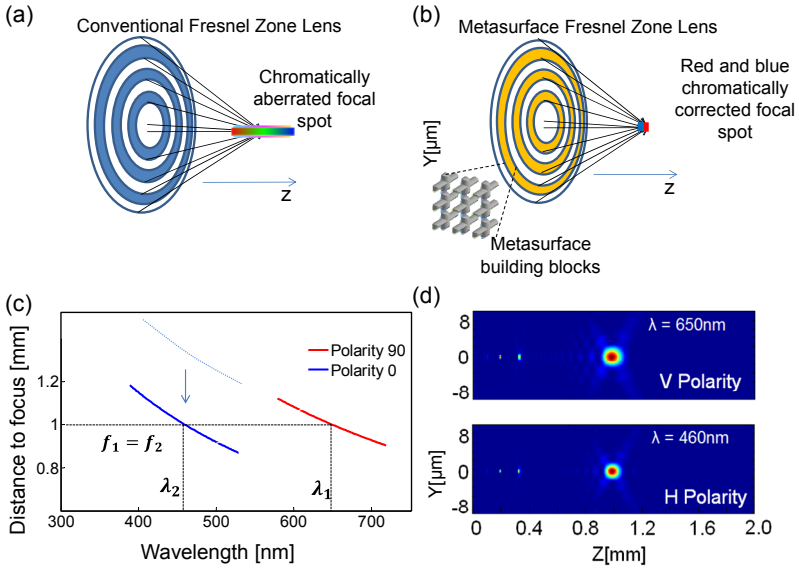

Fig. 2. Correcting chromatic aberrations at pairs of wavelengths with mFZP. (a) Conventional 2D FZP. Each wavelength has a different focal point. (b) Suggested FZP based on metasurface that reduces the chromatic aberrations by focusing pairs of wavelengths to the same focal spot. (c) Focal distance vs. wavelength of mFZP designed to focus 650 nm and 460 nm light to 1 mm focal distance. (d) Beam propagation simulation results of operation of mFZP at wavelength of 650 nm with vertical polarization and wavelength of 450 nm with horizontal polarization. Both wavelengths focus to 1 mm away from the lens.

To demonstrate experimentally the operation of the proposed binary- amplitude mFZP we fabricated samples based on subwavelength arrays of rod- and cross- shaped aluminum (Al) ONATS on glass. The dimensions of the fabricated resonators were chosen after simulating the spectral transmission properties of arrays of rod and cross shaped ONATs that had widths of 40nm, thicknesses of 40nm and lengths varying between 90 nm to 200 nm. The vertical rod ONATs were designed to block light at 650 nm and the horizontal rod ONATS were designed to block light at 460 nm. In the places of overlap of the blocking regions of the two polarizations we placed anisotropic cross ONATS which were designed to operate at the corresponding wavelengths as the rod ONATs of the same orientation, i.e. one arm of the crosses was designed to block light at 650 nm and the other was designed to block light at 460 nm. The polarized dual-band behavior therefore is obtained at the level of the unit cell. The samples were fabricated by standard electron beam lithography. The dimensions of the vertical ONATs were 180 nm × 40 nm, 40 nm thick and the pitch was 200 nm. The horizontal ONATs were 100 nm × 40 nm, 40 nm thick and the pitch was 280 nm. The cross shape ONATs shared the same parameters.

#228831 - $15.00 USD Received 9 Dec 2014; revised 18 Jan 2015; accepted 19 Jan 2015; published 9 Feb 2015

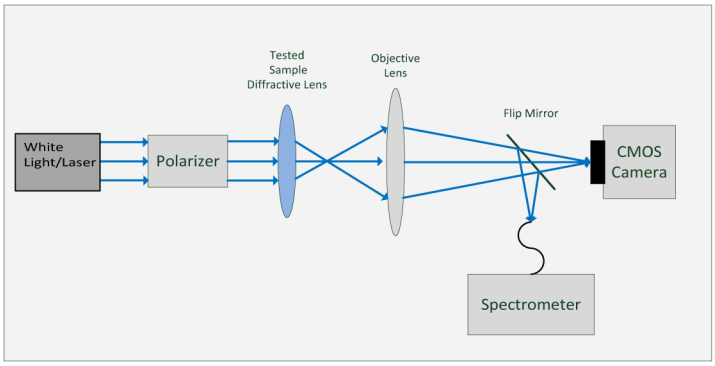

Fig. 3. Test setup for dual wavelength mFZP. For the light source, we used white incoherent light (Xenon arc lamp) or tunable laser.

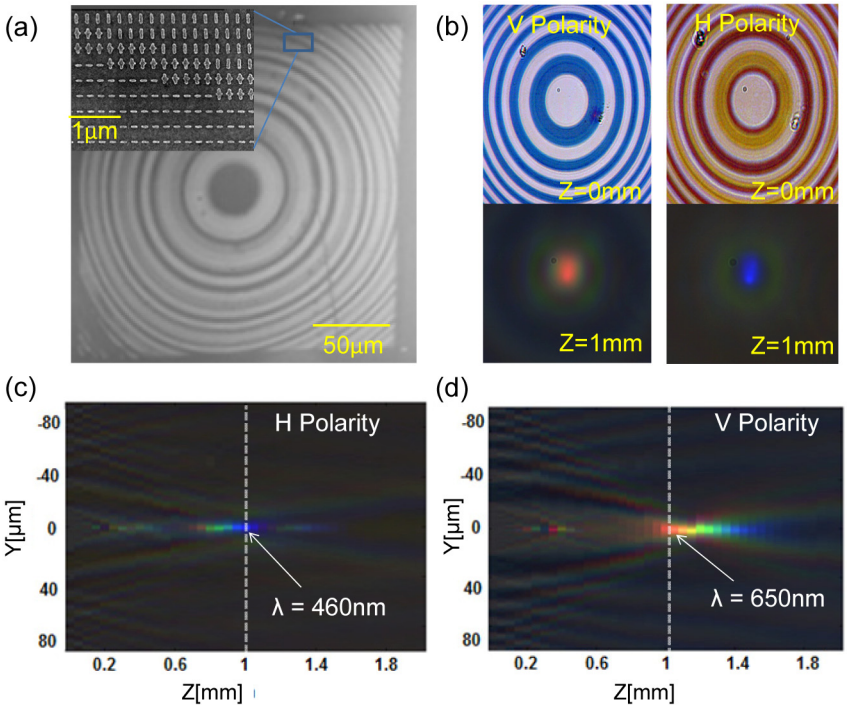

Fig. 4. Focusing results of mFZP lens. (a) SEM images of the fabricated mFZP. The inset shows an enlarged portion of the lens. (b) Optical images of the mFZP and corresponding focal spot at 1 mm at two different polarizations. (c) Measurements of light propagation after the mFZP at distances of 0 to 2 mm with horizontally polarized white light and (d) with vertically polarized light.

To examine the samples optically we used a home built transmission microscope setup [Fig. 3]. Figure 4(a) shows a scanning electron microscope (SEM) image of the fabricated mFZP. The mixture of the three types of ONATs can be seen in the inset. Figure 4(b) shows images of the operation of the fabricated mFZP tested with incoherent polarized white light from a Xenon arc lamp. The top two images are optical images of the lens at the two polarizations. It can be seen how different polarizations 'see' different lenses. At vertical polarization the lens appears blue since it blocks light in the red part of the spectrum (designed for 650 nm wavelength) and at horizontal polarization the lens appear yellow-red due to blocking of light at the blue part of the spectrum (designed for 460 nm wavelength).

#228831 - $15.00 USD Received 9 Dec 2014; revised 18 Jan 2015; accepted 19 Jan 2015; published 9 Feb 2015

The lens does not appear at a uniform color at this polarization due to red shift of the resonances of the fabricated rod shaped ONATs compared to the cross shaped ONATs. The bottom images show the focal spot 1 mm away from the lens demonstrating that the two different polarizations focus different colors. In order to examine the propagation of light away from the lens we used the same method that was used to examine the 1D FZP. Figures 4(c) and 4(d) are built from a sequence of images taken at different distances from the lens. The step between each of the images is 0.05mm. It can be seen how according to the design, light at two different colors is indeed focused to the same spot in space.

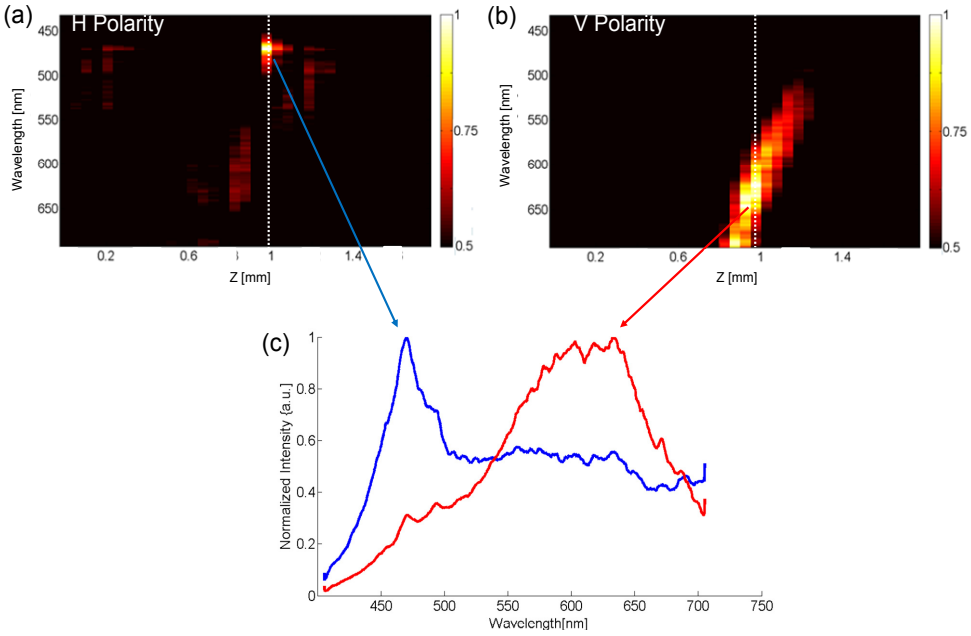

Fig. 5. Spectral measurements of on axis light distribution after the fabricated mFZP. (a) With horizontally polarized white light and (b) with vertically polarized light. Values above half maximum are shown to reduce noises due to fabrication imperfections. (c) Normalized light intensity at the focal distance (1mm). Red line shows the vertical polarization, and blue line shows the horizontal polarization.

The functionality of the mFZP depends on the wavelength acceptance of the ONATs. Since there is an operation bandwidth for the ONATs other wavelengths also respond. This is shown as the wavelengths that are focused away from 1 mm. Figure 5 shows spectral measurements (Andor Shamrock 303i) of the on-axis light distribution after the lens for the two polarizations. Figure 5(a) with horizontally polarized white light and Fig. 5(b) with vertically polarized light. The white line marks the focal distance of 1mm from the lens. With horizontally polarized white light we achieved focusing of wavelengths around 460nm, and with vertically polarized white light we achieve focusing of wavelengths around 650nm light (red). Figure 5(c) illustrates the normalized light intensity at the focal distance of 1mm from the lens for both light polarizations. In order to have good wavelength selectivity of the lens it is beneficial to use configurations which impose sharp resonance on the ONATs that compose the metasurface. Nevertheless the Al ONAT based mFZP that was tested operates according to its design shown in Figs. 2(c) and 2(d) and corrects the chromatic aberrations at pairs of wavelengths accordingly.

The demonstrated lenses can be used for applications where pairs of wavelengths need to be focused to the same point in space. To examine it, we tested the lens operation under coherent illumination as well. Figure 6 shows the polarized images of the lens and the

#228831 - $15.00 USD Received 9 Dec 2014; revised 18 Jan 2015; accepted 19 Jan 2015; published 9 Feb 2015

focusing by the lens when illuminated with coherent light ($\lambda = 460\,nm, \lambda = 650\,nm$; Chameleon OPO VIS). It can be seen that both wavelengths focus to 1 mm, however the blue beam has an additional focus at ~1.4 mm due to imperfection of the fabrication. This imperfection can be seen also in Fig. 6(a) for the horizontal polarity, showing that some of the blocking zones are much thinner than the others. By correcting this fabrication imperfection the additional blue focus at 1.4mm will be eliminated.

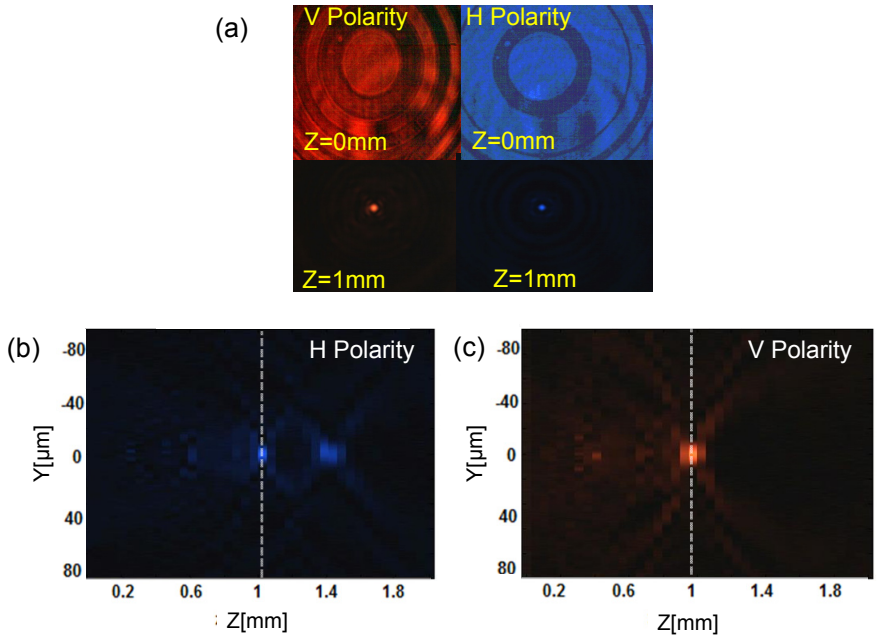

Fig. 6. Focusing measurements of dual wavelength mFZP lens with coherent light illumination. (a) Images of the lens and focal spot at two different polarizations and two different laser wavelengths. On the left using vertically polarized light at 650nm and on the right hand side using horizontally polarized light at 460nm. (b) Blue light propagation (wavelength of 460 nm) after the lens for horizontally polarized light. Two focal points were measured due to a mismatch in the transmission response of the horizontal rod shape antennas and the horizontal part of the cross shape antennas. (c) Red light propagation (wavelength of 650 nm) after the lens for vertically polarized light.

Conclusion

In conclusion, we show here that nanostructured metasurfaces composed of tightly packed ONATs can be used as new means to design DOEs which correct chromatic aberrations at pairs of wavelengths. We specifically demonstrated experimentally an mFZP which can focus blue and red light to the same point in space. This mFZP can be used as an ultrathin lens for a variety of applications that require a single focal point for pairs of wavelengths including fluorescence imaging where both excitation wavelength and emission wavelength have to share the same focal spot or for stimulated emission depletion microscopy where the pump beam and the depletion beam have to share focus. Our method can be extended by using multilayer and multi-wavelength design towards generating DOEs for multispectral imaging. The use of a multilayer structure as suggested in [30] can reduce the metasurface reflection and improve the overall efficiency of the lens. In addition hybrid refractive/diffractive optical elements can be designed for extended aberration correction. Moreover, this method can be used to make dual wavelength plasmonic holograms [2,26,28,31] in order to achieve

#228831 - $15.00 USD Received 9 Dec 2014; revised 18 Jan 2015; accepted 19 Jan 2015; published 9 Feb 2015

multicolor functionality. We therefore believe that this work opens new possibilities to use DOEs in various applications.

Acknowledgments

This work was supported mainly by the Israeli Ministry of Trade and Labor – Kamin Program, grant. No. 51387 and was partially supported by the Israeli Science Foundation, grant no. 133113.

#228831 - $15.00 USD Received 9 Dec 2014; revised 18 Jan 2015; accepted 19 Jan 2015; published 9 Feb 2015